

# Reaction4Exp commented example: ${}^4\text{He} + {}^{208}\text{Pb}$ elastic scattering

## Introduction

This document describes briefly the use of the Reaction4Exp website for the case of elastic scattering. We will use as example the  ${}^4\text{He} + {}^{208}\text{Pb}$  reaction. The link to the elastic scattering website is:

<https://reaction4exp.us.es/elastic/index.php>

## 1 Reminder of the optical model

In the optical model, the projectile-target interaction is described by means of an effective interaction,  $U(\mathbf{R})$  (the *optical potential*). The scattering wavefunction, that describes the relative motion between the projectile and target, is a solution of a single-channel Schrodinger equation:  $[H - E]\Psi(\mathbf{R}) = 0$  where  $E$  is the CM energy. This solution is conveniently expanded in spherical harmonics. For a *central potential* (i.e.  $U = U(R)$ ) and *ignoring intrinsic spins*, this yields:

$$\Psi(\mathbf{K}, \mathbf{R}) = \frac{1}{KR} \sum_L (2L+1) i^L \chi_L(K, R) P_L(\cos \theta), \quad (1)$$

where  $\theta$  is the angle between the incident momentum  $\mathbf{K}$  and the final momentum  $\mathbf{K}'$ , which corresponds to the scattering angle in the c.m. frame.

The radial functions  $\chi_L(K, R)$  are determined inserting this expansion into the Schrödinger equation, giving rise to an equation for each value of  $L$ ,

$$\left[ \frac{\hbar^2}{2\mu} \frac{d^2}{dR^2} - \frac{\hbar^2}{2\mu} \frac{L(L+1)}{R^2} - U(R) + E \right] \chi_L(K, R) = 0, \quad (2)$$

where  $U(R)$  contains both the Coulomb and nuclear potentials.

The above Schrödinger equation is solved numerically from  $R = 0$ , starting from the value  $\chi_L(K, 0) = 0$ , and up to a maximum value (*matching radius*)  $R_{\max}$ . At this distance, one imposes the boundary condition:

$$\chi_L(K, R)|_{R=R_{\max}} = \frac{i}{2} e^{i\sigma_L} \left[ H_L^{(-)}(\eta, KR_{\max}) - S_L H_L^{(+)}(\eta, KR_{\max}) \right] \quad (3)$$

where  $\sigma_L$  are the Coulomb phase-shifts and  $H_L^{(\pm)}(\eta, KR)$  are the ingoing ( $-$ ) and outgoing ( $+$ ) Coulomb functions. From the condition (3), one determines the coefficients  $S_L$  ( $S$ -matrix elements) which, in turn, are used to compute the elastic scattering amplitude:

$$f(\theta) = f_C(\theta) + \frac{1}{2iK} \sum_L (2L+1) e^{2i\sigma_L} (S_L - 1) P_L(\cos \theta) \quad (4)$$

where  $f_C(\theta)$  is the scattering amplitude for pure Coulomb scattering (whose square is the Rutherford cross section).

The differential elastic cross section is evaluated according to

$$\frac{d\sigma}{d\Omega}(\theta) = |f_C(\theta) + f_N(\theta)|^2. \quad (5)$$

An important quantity is the reaction cross section, which is associated with the flux of all non-elastic channels. In terms of the  $S$ -matrix elements it is given by:

$$\sigma_{\text{reac}} = \frac{\pi}{K^2} \sum_L (2L+1)(1 - |S_L|^2) \quad (6)$$

where  $K$  is the cm wave number.

## 2 Optical model parameters

The projectile-target interaction is the sum of the Coulomb and the nuclear potentials. For the Coulomb potential, the Reaction4Exp tool uses the Coulomb interaction for a uniformly charged sphere:

$$V_c(r) = \begin{cases} \kappa \frac{Z_1 Z_2 e^2}{2R_c} \left(3 - \frac{r^2}{R_c^2}\right) & \text{if } r \leq R_c \\ \kappa \frac{Z_1 Z_2 e^2}{r} & \text{if } r \geq R_c \end{cases}$$

where  $R_c$  is related to the sum of the charge radii of the colliding nuclei. Instead of using  $R_c$  directly, the Reaction4Exp website uses the so-called reduced radius,  $r_c$ , which is related to the physical radius as  $R_c = r_c(A_1^{1/3} + A_2^{1/3})$ , as is standard. In our working example  $A_1 = 4$  and  $A_2 = 208$ .

For the nuclear part, we consider the following parametrization in terms of *volume* Woods-Saxon shapes, which is in fact the standard choice in the Reaction4Exp website:

$$U_{\text{nuc}}(r) = -V_0 f(r, R_0, a_0) - iW_v f(r, R_i, a_i),$$

with

$$f(r, R_x, a_x) = \{1 + \exp[(r - R_x)/a_x]\}^{-1}$$

We will adopt the numerical values listed in table 2. In the website, reduced radii are introduced. Then, these are converted internally to absolute (physical) radii using the projectile and target atomic numbers:  $R_x = r_x(A_p^{1/3} + A_t^{1/3})$ .

Figure 1 shows a screenshot of the OM parameters section in the Reaction4Exp website.

### 2.1 Numerical integration parameters

In addition to the optical potentials, we need to specify some additional parameters required for the numerical integration of the radial equation. Although the application

System	$V_0$ [MeV]	$r_0$ [fm]	$a_0$ [fm]	$W_v$ [MeV]	$r_i$ [fm]	$a_i$ [fm]	$r_c$ [fm]
${}^4\text{He}+{}^{208}\text{Pb}$	96.44	1.085	0.625	32	0.958	0.42	1.2

Table 1: Woods-Saxon parameters for  ${}^4\text{He}+{}^{208}\text{Pb}$  optical model. Reduced radii ( $r_x$ ) are converted into absolute (physical) radii as  $R_x = r_x(A_p^{1/3} + A_t^{1/3})$ .

**$A_p$  and  $A_t$  for radii conversion**

$R_0 = r_0(A_p^{1/3} + A_t^{1/3})$      $A_p$       $A_t$

**Generate potential**

**Coulomb potential**

$r_c$  (fm)     Switch off Coulomb ☐

**Nuclear potential**

Type	Shape	$V_0$ (MeV)	$r_0$ (fm)	$a_0$ (fm)	$W_0$ (MeV)	$r_i$ (fm)	$a_i$ (fm)
Volume, central potential	Woods-Saxon	120	1.25	0.65	50	1.25	0.65

**Potential parameters**

- $A_p$  and  $A_t$  for radii conversion
- $r_c$ : reduced Coulomb radius.
- $V_0$ : Depth of real volume optical potential.
- $r_0$ : Reduced radius for real volume optical potential.
- $a_0$ : Diffuseness of real volume optical potential.

Figure 1: Optical parameters section of the Reaction4Exp website.

sets some default values, it is convenient to check that the calculations are *converged* with respect to these parameters. In the Reaction4Exp website, we need to specify the following numerical parameters:

- **Integration step ( $h$ ):** This is the radial step used for the numerical integration of the differential equation (2). It has to be chosen smaller than the diffuseness of the potentials and than the characteristic wavelength of the projectile. A simple criterion is to set  $hk \leq 0.2$ , where  $k$  is the wave number associated with the kinetic energy. For example, for  $E_{\text{lab}}=22$  MeV,  $k = 2.01 \text{ fm}^{-1}$  and so  $h \leq 0.2/2.01 = 0.1 \text{ fm}$ . If the integration step is too low for the considered energy, the website will show a notification. Note that too small values of  $h$  may lead to numerical instabilities.
- **Matching radius.** This is the distance up to which the radial equations (2) are integrated. Beyond the matching radius, the code will assume that all interactions (but the monopole Coulomb one) have vanished and so the wavefunction has reached its asymptotic behaviour, given by Eq. (3). Thus, the matching radius must be chosen well outside the range of the optical potential. In our example, this potential extends up to  $\approx 10 \text{ fm}$ , so  $R_{\text{max}} \geq 20 \text{ fm}$  would be a “safe” choice. Note that too large values for the matching radius may lead to numerical issues.
- **Minimum and maximum total angular momentum.** The total angular momentum is the sum of the orbital angular momentum  $L$  and the spins of projectile and target:  $\vec{J}_T = \vec{L} + \vec{J}_p + \vec{J}_t$ . In principle, the sum in  $L$  of Eq. (4) goes from 0 to infinity. Therefore the minimum value of the angular momentum should be set to 0 unless there is some interest in visualizing the effect of low values of  $L$ . (Even if the vector coupling  $\vec{J}_p + \vec{J}_t$  is half-integer, so  $J_T$  is half-integer and its minimum value 0.5, setting the minimum value to 0 will be properly recognized by the program). In practice, convergence of the scattering observables is achieved for finite values of  $L$  since, for large values of  $L$ ,  $S_L \rightarrow 1$  and hence these values do not contribute to the sum (4). This occurs because, for large partial waves, the nuclear potential is negligible and the corresponding nuclear phase-shift tends to zero.

Clearly, the maximum value of  $L$  must be larger than the “grazing” angular momentum ( $L_g$ ), i.e., the value of  $L$  corresponding to classical trajectories for which the nuclei start to feel the nuclear interaction. When the Coulomb force is weak,  $L_g$  can be estimated from the relation between the impact parameter and the angular momentum for a classical trajectory<sup>1</sup>:

$$\sqrt{L(L+1)} \approx L + \frac{1}{2} \simeq kb. \quad (7)$$

---

<sup>1</sup>This expression arises from the relation between the impact parameter and the angular momentum in a classical trajectory due to a central potential, i.e.,  $|\vec{L}| = m v b = p b$ . In quantum mechanics the modulus of the angular momentum is  $\sqrt{L(L+1)}\hbar$  and the linear momentum is related to the wave number by  $p = \hbar k$ . Then, the relation above becomes  $\sqrt{L(L+1)} = kb$ .

Then,  $L_g$  is estimated setting  $b = R_g$ , where  $R_g$  is called “grazing” or critical radius, and corresponds to the distance at which the nuclei begin to experience the nuclear interaction. The value of  $R_g$  is found to be somewhat larger than the sum of the projectile and target radii ( $R_g > 1.2(A_p^{1/3} + A_t^{1/3})$  fm). A simple estimate is given by  $R_g \simeq 1.45(A_p^{1/3} + A_t^{1/3})$  fm. If the deflection due to the Coulomb interaction is important, instead of Eq. (7) we may use the relation between the angular momentum and the distance of closest approach  $r_{min}$  for a classical Coulomb trajectory:

$$\sqrt{L(L+1)} \approx L + \frac{1}{2} = kr_{min} \left[ 1 - \frac{2\eta}{kr_{min}} \right]^{1/2} \quad (8)$$

where  $\eta$  is the Sommerfeld parameter. Then, we estimate  $L_g$  as the angular momentum for which  $r_{min} = R_g$ . Expressions (7) and (8) tell us that the number of partial waves (that is, values of  $L$ ) involved in the calculation scales as the square root of the kinetic energy.

The asymptotic region will correspond to “trajectories” well beyond the grazing impact parameter so, ideally,  $J_T^{\max} \sim L_{\max} \gg L_g$ . This gives a hint to choose a suitable value of  $J_T^{\max}$ . In practice, one increases progressively  $J_T^{\max}$  until convergence of the studied observable is achieved. One can also verify that the reaction cross section has dropped to 0 for  $J_T^{\max}$ . Note that too large values for  $J_T^{\max}$  may lead to numerical problems in the calculation.

In some situations, we can estimate  $R_g$  (and hence  $L_g$  from the relations above) from the elastic angular distribution. This is the case of Fresnel and Fraunhofer scattering:

1. In **Fresnel** scattering,  $L_g$  is sometimes estimated as the value of  $L$  which satisfies  $|S_L|=0.5$ . Another common prescription is the *quarter-point* recipe. In this case, one determines a “grazing” angle,  $\theta_g$ , defined as the angle for which the elastic cross section drops to 1/4 of the Rutherford cross section. From this, one estimates the grazing angular momentum as

$$L_g + 1/2 \approx \eta \cot \left( \frac{\theta_g}{2} \right) \quad (9)$$

and  $R_g$  as the distance of closest approach for that Coulomb orbit:

$$R_g = \frac{\eta}{k} \left( 1 + \frac{1}{\sin(\theta_g/2)} \right) \quad (10)$$

2. In **Fraunhofer** scattering, the separation  $\Delta\theta$  of successive maxima or minima gives a measure of the grazing angular momentum,

$$\Delta\theta \approx \pi/L_g, \quad (11)$$

and then  $R_g$  can be estimated from  $kR_g \simeq L_g + 1/2$ . As in Fresnel scattering, another estimate of  $L_g$  can be obtained from the S-matrix as  $|S_{L_g}|=0.5$ .

**Figure 2 shows a screenshot of the R4E section for the numerical integration parameters.**

Reaction	Potentials	Integration Parameters
Radial grid (fm):	step (h) <input type="text" value="0.1"/>	Matching radius <input type="text" value="30"/>
Total angular momentum:	min <input type="text" value="0"/> max <input type="text" value="40"/>	
Angular range (degrees):	min <input type="text" value="1"/> max <input type="text" value="180"/>	step <input type="text" value="1"/>

**Integration parameters**

- **Radial step (h)** It has to be chosen smaller than the diffuseness of the potentials and than the characteristic wavelength of the projectile. A simple criterion is to set  $hk \leq 0.2$ , where  $k$  is the wave numbers associated with the kinetic energy ( $k = \sqrt{2 E_{cm} \mu} / \hbar$ ).
- **Matching radius** (for R > R<sub>MATCH</sub> asymptotic behaviour is assumed)

Figure 2: Numerical integration parameters section.

$E_{\text{lab}}$ (MeV)	$E_{\text{cm}}$ (MeV)	$k$ (fm <sup>-1</sup> )	$\eta$	$r_{\text{min}}$ (fm)
5	4.91	0.960	23.1	48.1
10	9.81	1.36	16.3	24.1
22	21.6	2.01	11.0	10.9
27	26.5	2.23	9.94	8.9
60	58.9	3.32	6.67	4.0

Table 2: Useful kinematical parameters for the  $^4\text{He} + ^{208}\text{Pb}$  reaction at several incident energies. The parameters  $k$ ,  $\eta$  and  $r_{\text{min}}$  correspond, respectively, to the wave number, the Sommerfeld parameter, and the distance of closest approach for a head-on collision.

### 3 Interpretation of the results

In Table 2 we list some kinematical parameters, namely, the wave number ( $k$ ), the Sommerfeld parameter ( $\eta$ ), and distance of closest approach in head-on Coulomb collision ( $r_{\text{min}}$ ). These quantities can be computed with the expressions,

$$k = \sqrt{\frac{2\mu E_{\text{cm}}}{\hbar^2}} = \sqrt{\frac{2\mu E_{\text{lab}}}{\hbar^2} \frac{A_t}{A_t + A_p}}; \quad \eta = \kappa \frac{Z_p Z_t e^2}{\hbar v} = \kappa \frac{Z_p Z_t e^2 \mu}{\hbar^2 k}; \quad r_{\text{min}} = \kappa \frac{Z_1 Z_2 e^2}{E_{\text{cm}}}$$

where  $\kappa = 1/(4\pi\epsilon_0)$ . Note that this expression is more easily evaluated in a system of units with  $\kappa = 1$ .

#### 3.1 Coulomb barrier

The nominal height of the Coulomb barrier can be estimated from the maximum of the real (Coulomb plus nuclear) potential. According to Fig. 3 we see that this is around 22 MeV. This is consistent with the simple estimate:

$$V_b \approx \frac{Z_1 Z_2 e^2}{R_b}; \quad R_b \approx 1.44(A_1^{1/3} + A_2^{1/3}) \text{ fm}$$

which, in this case, gives  $V_b \approx 21.8$  MeV and  $R_b = 10.8$  fm.

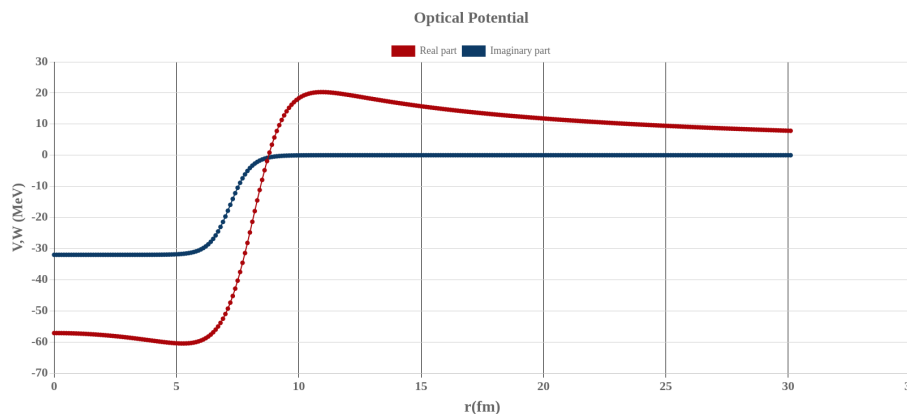


Figure 3: Real and imaginary parts of the optical potential, as displayed by the Reaction4Exp website.

### 3.2 Differential cross sections

The elastic differential cross section is shown in Fig. 4 for several incident energies: 10, 22, 27 and 60 MeV, plotted relative to the Rutherford cross section. We can see that:

- At  $E=10$  MeV, the ratio is almost 1, that is, we are in a situation of **pure Coulomb scattering** and is well described by the Rutherford formula. At this energy, the projectile does not *feel* the nuclear interaction. This is consistent with large value of  $r_{\min}$  listed in Table 2.
- At  $E=22$  MeV, the distribution departs from the Rutherford formula, as a consequence of the nuclear interaction. Beyond a certain angle ( $\theta_{\text{c.m.}} \approx 60^\circ$ ), the cross section drops quickly. This is typical of the “shadow” region observed in diffraction that occurs in Fresnel scattering.
- At  $E=27$  MeV, the elastic angular distribution displays a typical **Fresnel** diffraction pattern. We recall that a prerequisite for the observation of this pattern is that  $L_g \gg 1$  and  $\eta \gg 1$ . According to Table 2, at this energy  $\eta = 8.9$ , so the latter condition is fulfilled. The grazing angular momentum can be estimated from the condition  $|S_L| = 0.5$  which occurs for  $L \simeq 10$ .
- At  $E=60$  MeV, the angular distribution displays a more oscillatory structure, thus departing from the Fresnel pattern and approaching to what we have called **Fraunhofer** scattering.

### 3.3 $S$ -matrix elements

Reaction4Exp provides also the nuclear  $S$ -matrix<sup>2</sup>, which is related to the coefficient of the outgoing waves for a given partial wave  $L$  [see Eq. (3)]. This is usually expressed

<sup>2</sup>More precisely, the Coulomb modified nuclear  $S$ -matrix

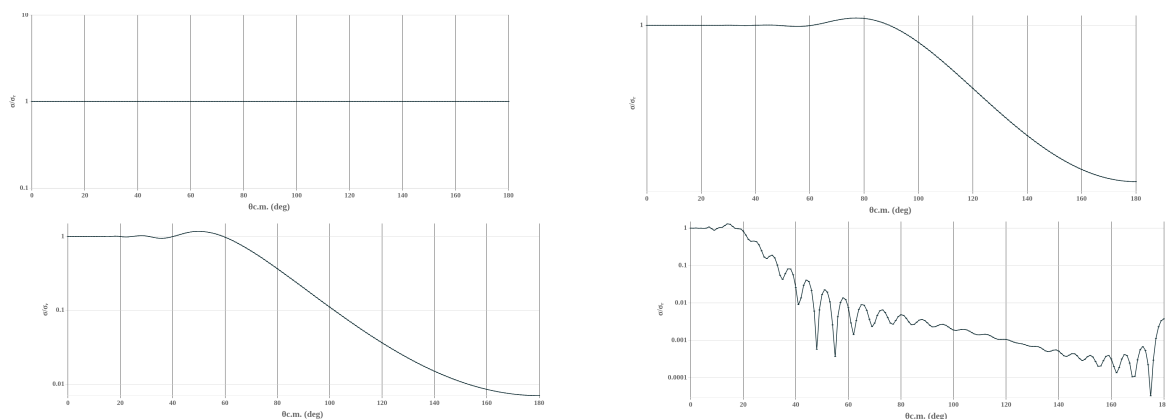


Figure 4: Elastic differential cross sections relative to Rutherford cross section at  $E_{lab}=10, 22, 27$  and  $60$  MeV (from left to right and top to bottom).

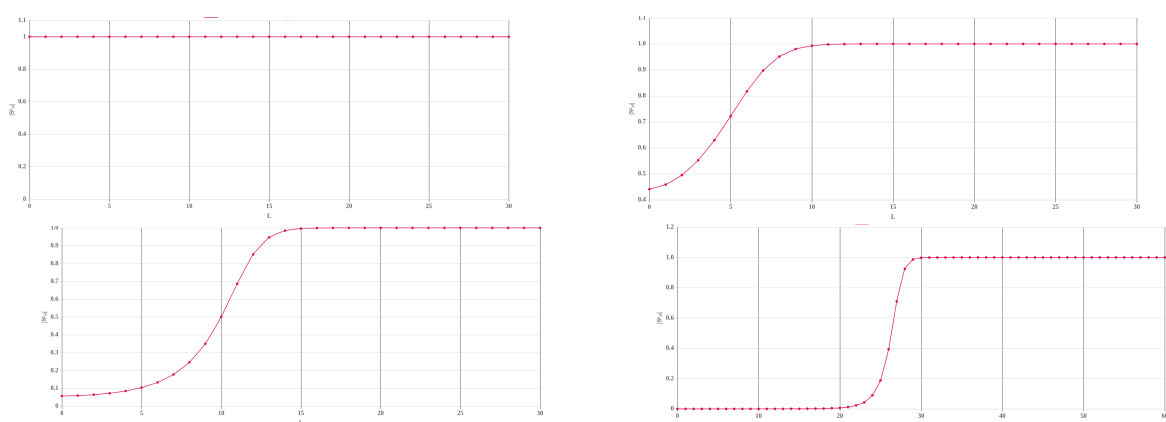


Figure 5: Modulus of the elastic S-matrix as a function of the total angular momentum  $J_T$  for energies  $E_{lab}=10, 22, 27$  and  $60$  MeV (from left to right and top to bottom).

as

$$S_L = e^{2i\delta_L},$$

where  $\delta_L$  are the *phase shifts* of the  $L$ th partial wave. Let us recall some properties of the  $S$ -matrix and their associated phase shifts:

- In absence of nuclear potentials  $\delta_L = 0$  and  $S_L = 1 \forall L$
- If there are only real potentials,  $|S_L| = 1 \forall L$ .
- When an imaginary potential is present,  $|S_L| < 1$  for small  $L$  but, for large  $L$ ,  $|S_L| \rightarrow 1$ .

The fact that  $|S_L| < 1$  for small values of  $L$  reflects the loss of flux caused by the imaginary potential. Classically, it can be understood through the relation (7) and (8). Small impact parameters correspond to closer trajectories, and hence to a higher sensitivity to the short-range potentials.



The Reaction4Exp website provides the modulus of the  $S$ -matrix. As an example, we plot in Fig. 5, the modulus of the  $S$ -matrix at four different energies: 10, 22, 27 and 60 MeV. We see that:

- At  $E = 10$  MeV, the modulus is almost 1 for all partial waves. This is telling us that there is no effect from the nuclear potential.
- At  $E=22, 27$  and 60 MeV, there is a range of values of  $L$  for which  $|S_L| < 1$ . Moreover, this absorptive effect becomes more important for increasing incident energy.
- The range of values of  $L$  for which  $|S_L| < 1$  increases for increasing energy. This can be understood as the increase of the grazing angular momentum with increasing incident energy, according to Eq. (7).

Reaction4Exp also provides the Argand plot and the phaseshifts as a function of  $J$ , but they will not be discussed at this point.

### 3.4 Near-side and far-side decomposition of the elastic cross section

In addition to the elastic cross section the Reaction4Exp website provides also the *nearside* and *farside* components. In Fig. 6 this decomposition is shown for the 3 energies considered above. We can see that:

- At 10 and 27 MeV, the cross section is almost entirely due to the nearside trajectories.
- At  $E=60$  MeV, there are smooth regions dominated by either the *nearside* or the *farside* components. However, around  $\theta_{\text{cm}} \approx 60^\circ$  and  $\theta_{\text{cm}} \approx 170^\circ$  both components have similar magnitude, and their interference produces the observed oscillations in the elastic scattering.

## 4 Classical description of the reaction

In the Reaction4Exp website it is possible to perform classical calculations for elastic scattering by selecting “Classical model”. The inputs (reaction and potential) are the same as those for the optical calculation, and, if already input, will be copied from the Optical Model section to the Classical Model one. It is advisable to check that the input are the expected ones.

This calculation results in various outputs, providing the turning point of the trajectory, the scattering angle (deflection function) and the survival probability as a function of the impact parameter as well as a sample of the trajectories in the center of mass, which is useful to visualize the rainbows and particularly the orbiting.

Figures 8 and 9 present the deflection function and survival probability respectively for the reaction at 10, 22, 27 and 60 MeV. It is visible that while for 10 MeV, the

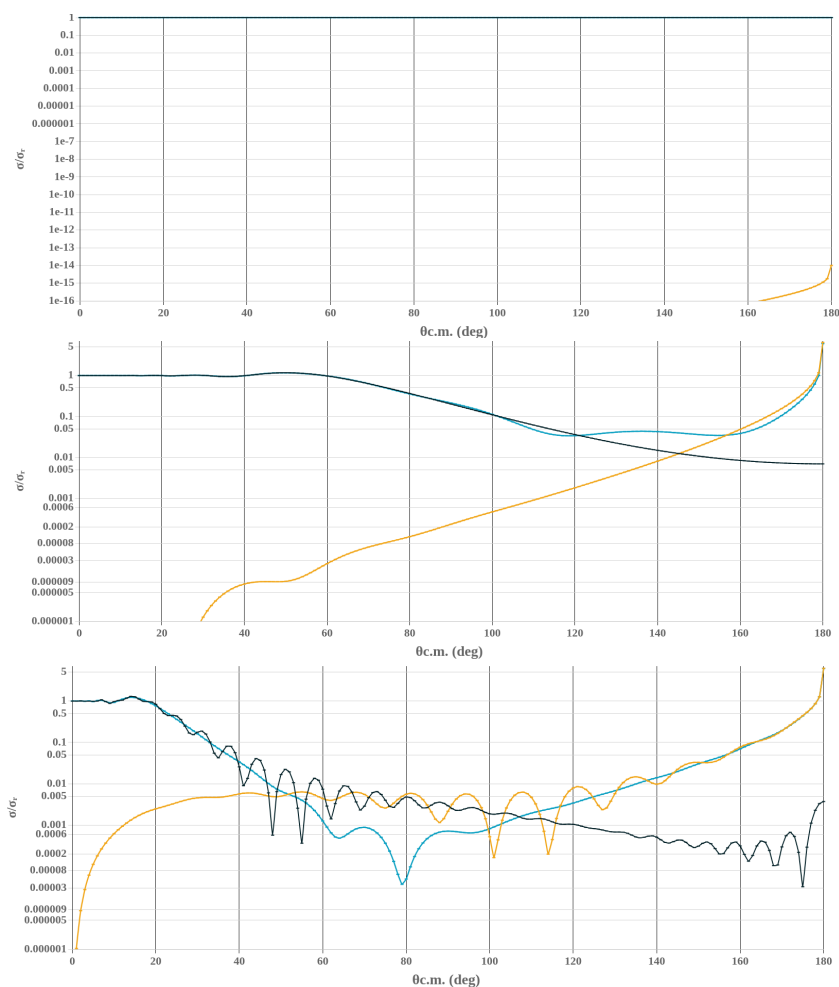


Figure 6: Far-side /near-side decomposition of the elastic cross section  ${}^4\text{He}+{}^{208}\text{Pb}$  at  $E_{\text{lab}}=10, 27$  and  $60$  MeV (top to bottom).

ELASTIC SCATTERING

Optical Model
Classical Model

Reaction
Potentials

Projectile  
 Target  
 Elab(MeV)

Nucleus	A	J	Parity
<div style="border: 1px solid #ccc; padding: 2px; display: flex; align-items: center;"> <span style="font-size: 0.8em; margin-right: 5px;">Select</span> <span style="font-size: 0.8em;">▼</span> </div>	<div style="border: 1px solid #ccc; width: 60px; height: 20px;"></div>	<div style="border: 1px solid #ccc; width: 60px; height: 20px;"></div>	<div style="border: 1px solid #ccc; padding: 2px; display: flex; align-items: center;"> <span style="font-size: 0.8em; margin-right: 5px;">+1</span> <span style="font-size: 0.8em;">▼</span> </div>
<div style="border: 1px solid #ccc; padding: 2px; display: flex; align-items: center;"> <span style="font-size: 0.8em; margin-right: 5px;">Select</span> <span style="font-size: 0.8em;">▼</span> </div>	<div style="border: 1px solid #ccc; width: 60px; height: 20px;"></div>	<div style="border: 1px solid #ccc; width: 60px; height: 20px;"></div>	<div style="border: 1px solid #ccc; padding: 2px; display: flex; align-items: center;"> <span style="font-size: 0.8em; margin-right: 5px;">+1</span> <span style="font-size: 0.8em;">▼</span> </div>

Elab(MeV)

**Reactions parameters**

- Elab: Incident laboratory energy.
- J: projectile and target angular momentum.

**CALCULATE**

[Upload input from extern file](#)

Figure 7: Elastic scattering input website, with the Classical Model option selected

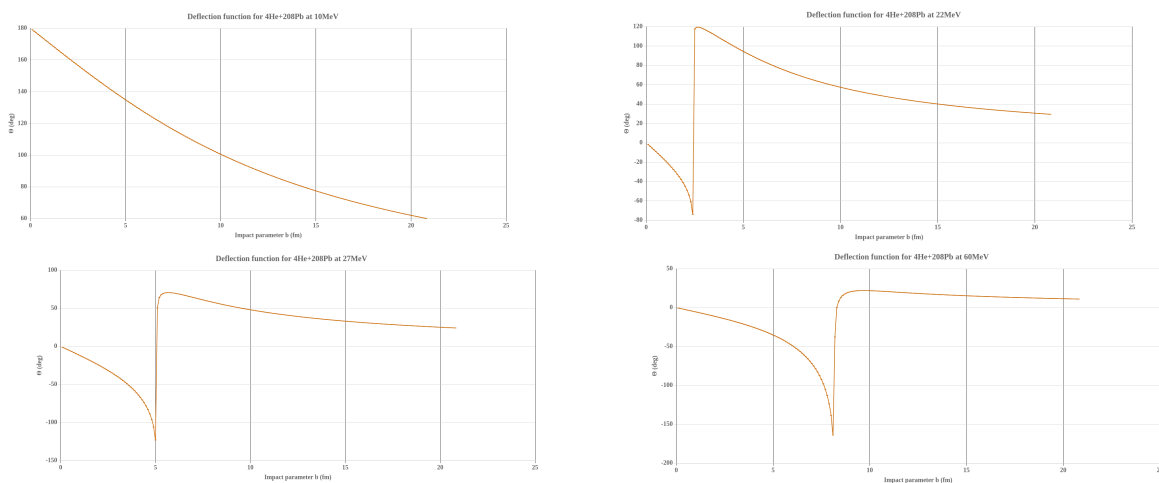


Figure 8: Deflection function for energies  $E_{\text{lab}}=10, 22, 27$  and  $60$  MeV (from left to right and top to bottom).

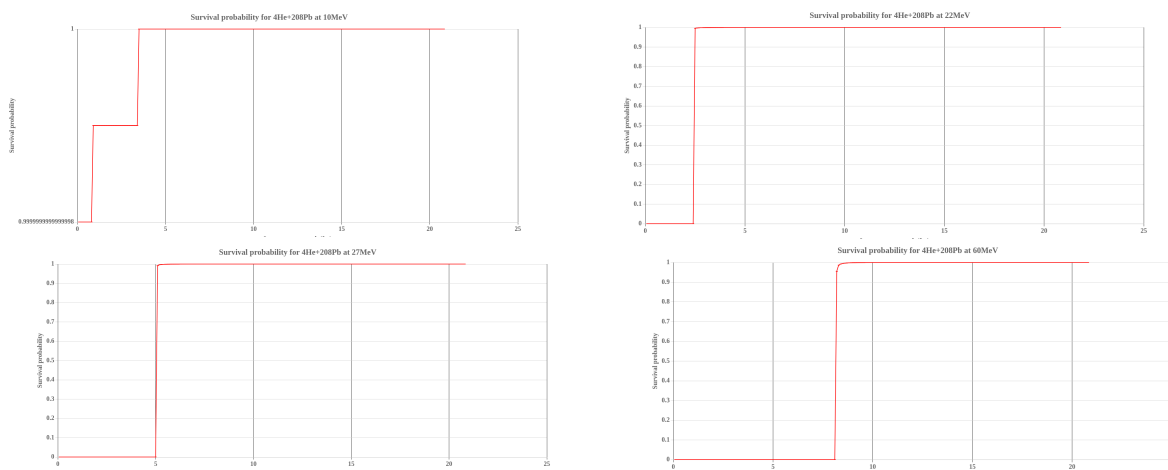


Figure 9: Survival probability for energies  $E_{\text{lab}}=10, 22, 27$  and  $60$  MeV (from left to right and top to bottom).

trajectories are Rutherford ones without absorption (note the labels in the Y axis for the survival probability), for energies over the Coulomb barrier, a rainbow and orbiting appear. It is very notable that this reaction occurs in a strong absorption regime, as seen by the sharp drop of survival probability at a certain impact parameter, which corresponds to the orbiting radius, due to the small velocity of the projectile in the orbiting region, which extends the interaction time between projectile and target and thus the absorption probability.

Reaction4Exp also provides an approximation for the rainbow angle considering a second-order approximation for the deflection function in a Fresnel regime. It is worth comparing this approximation with the maximum in the optical potential calculation. As expected, at high energies, with Fraunhofer scattering, the position of the rainbow is not well described by this approximation.